Functionalized electron-rich pyridines as initiators for the epoxy homopolymerization

David Edinger [1,2] ● Susanne M. Fischer [1,2] ● Christian Slugovc [1,2,*]

[1] Institute for Chemistry and Technology of Materials, Technische Universität Graz, Stremayrgasse 9, 8010 Graz, Austria, e-mail: slugovc@tugraz.at

[2] Christian Doppler Laboratory for Organocatalysis in Polymerization, Stremayrgasse 9, 8010 Graz, Austria

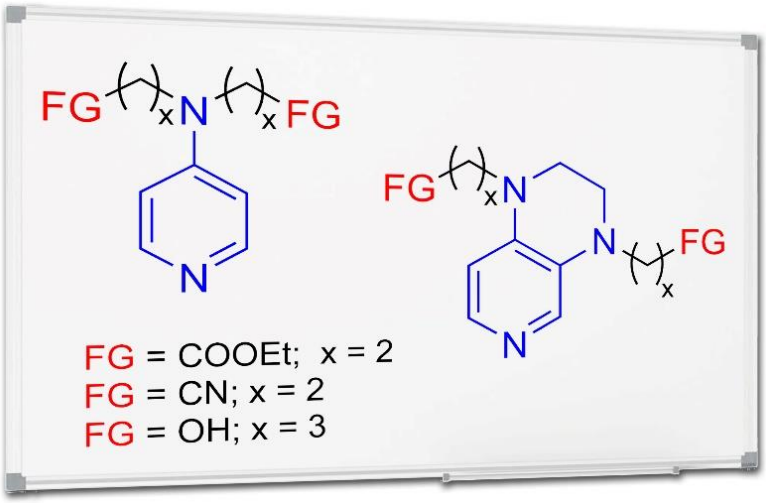

A simple and modular dialkylation of two electron-rich pyridine derivatives, namely 4-aminopyridine or 1,2,3,4-tetrahydropyrido[3,4-b]pyrazine, is achieved by aza-Michael reactions with electron-poor olefins (ethyl acrylate and acrylonitrile). Reducing the ester groups in the ethyl acrylate-derived compounds yielded the corresponding hydroxyl-containing derivatives. Subsequently, homopolymerization of phenyl glycidyl ether as well as an epoxy-alcohol polyaddition were catalyzed using the introduced compounds. As a reference catalyst, 4-dimethylaminopyridine was used. We found that in all cases an irreversible termination of the polymerization at temperatures above 100 °C occurred. The decomposition was particularly rapid in the case of pyridine derivatives containing hydroxyl groups. In contrast, at a constant temperature of 100 °C, the latter compounds gave the fastest phenyl glycidyl ether homopolymerization and high conversions were found for all electron-rich pyridine derivatives. However, testing the catalysts at high alcohol concentrations at temperatures higher than 100 °C resulted in similarly moderate conversions in all cases.

Introduction

4-(Dimethylamino)pyridine (DMAP) and related Lewis bases are widely used reagents for acylation, alkylation, condensation and transesterification reactions [1,2]. In polymer chemistry, DMAP is used as catalyst/initiator for living ring opening polymerization of lactide [3], in the conversion of isocyanates with alcohols [4] or as the initiator for aza- [5] and oxa-Michael polymerizations [6,7,8,9]. Further, DMAP is used in the homopolymerization of epoxy monomers [10,11] and in the combined polymerization of epoxy monomers and esters [11,12,13,14,15] as well as in the carbon dioxide addition to epoxides [16,17] and in the ring opening polymerization of cyclic carbonates [18]. In these cases, the use of DMAP often suffers from its poor solubility in the formulations. Since the use of solvents is usually undesirable, there is a strong interest to develop an easy and modular synthetic route to prepare DMAP analogues with tunable solubility. Another motivation is to provide a convenient method for incorporating additional functional groups, such as those used for polymerization or immobilization of DMAP derivatives [19,20], or for tuning the activity of the catalysts.

Herein we disclose a synthetic methodology based on the aza-Michael reaction [21] of 4-aminopyridine or 1,2,3,4-tetrahydropyrido[3,4-b]pyrazine with electron-poor olefins, namely acrylonitrile and ethyl acrylate, and test the performance of the obtained derivatives and their follow-up products (Scheme 1) in epoxy homopolymerization as well as in the epoxy-alcohol reaction. In this context, we are particularly interested in discovering the activity of electron-rich pyridines with additional hydroxyl groups, which, as will be shown, are easily accessible via the synthetic route discussed.

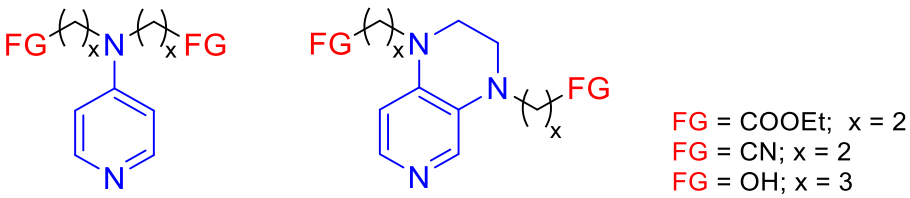

Scheme 1

DMAP is usually prepared by reacting dimethylamine with 1-(4-pyridyl)pyridinium chloride, which is accessible from pyridine and chlorine [22].

In contrast, here we start from 4-aminopyridine, accessible either via ammonolysis of 1-pyridylpyridinium dichloride or via a Hofmann rearrangement of the corresponding pyridinecarboxamide [23] and perform an aza-Michael reaction for the alkylation. This synthetic approach should also be readily applicable to the derivatization of other more complex electron-rich aminopyridines, as exemplified here by the synthesis of alkyl-substituted 3,4-diaminopyridines [24].

Results and Discussion

Firstly, the use of acrylonitrile as electron-poor olefin was investigated in the synthesis of the doubly cyanoethylated aminopyridine derivative (**1a**). Compound **1a** is readily obtained by heating 4-aminopyridine in acrylonitrile at 80 °C for 24 h in 68 % yield (Scheme 2). The synthesis of **1a** has been described in the literature using the same synthetic approach, but higher yields have been reported [25,26]. Compound **1a** has been used as an intermediate in the preparation of polymeric acylation catalysts [27]. A single crystal X-ray structure of **1a** is available [25].

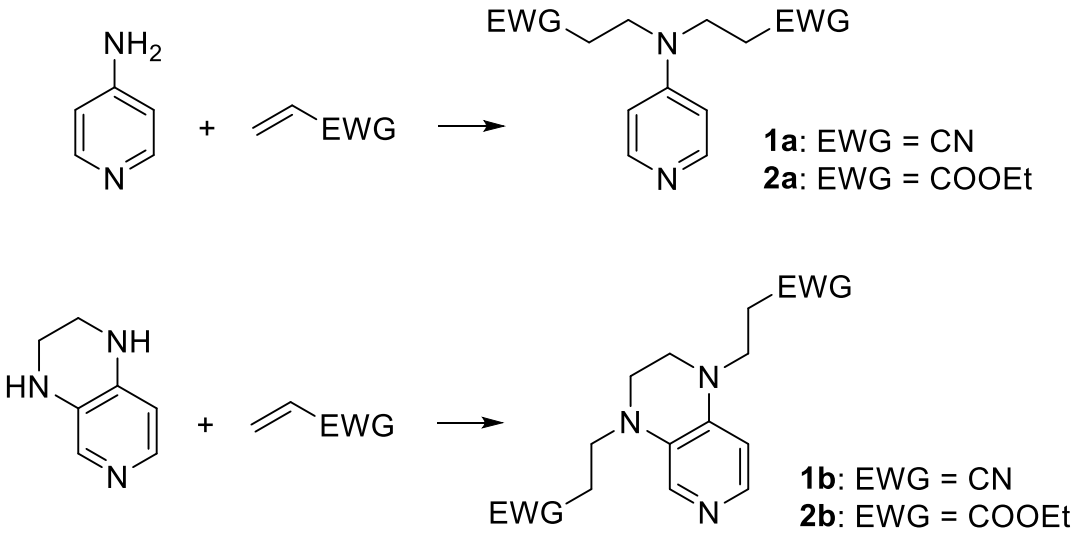

Scheme 2

In contrast, 3,3′-(2,3-dihydropyrido[3,4-b]pyrazine-1,4-diyl)bis[propanenitrile] (**1b**) is a previously unknown compound, which was prepared by heating a dispersion of 1,2,3,4-tetrahydropyrido[3,4-b]pyrazine in acrylonitrile for 24 h at

80 °C. Upon removal of volatiles an oily brown residue remained from which **1b** was isolated by column chromatography in 61 % yield.

Changing to ethyl acrylate as the Michael-acceptor, *N*-(3-ethoxy-3-oxopropyl)-*N*-4-pyridinyl-β-alanine ethyl ester (**2a**) was obtained in 43% yield by reacting 4-aminopyridine and ethyl acrylate at 80°C for 24 h. Compound **2a** has been previously disclosed in a patent [28] and the corresponding dimethyl ester derivative is also known [27,29,30]. The moderate yield is due to the need to separate ethyl acrylate oligomers by column chromatography. One of these by-products was obtained in pure form and was identified as **2a'** (Figure 1). In contrast to **2a**, the ^{1}H-NMR spectrum of **2a'** shows the presence of three ethyl ester groups (CH_2 at 4.2-4.1 ppm and CH_3 1.27-1.16 ppm) per pyridine moiety, rather than two as in **2a**. The 2-substituted pentanedioate substructure gives rise to a multiplet with the relative intensity of one proton at 2.83 ppm and two multiplets at 2.33 and 1.89 ppm. **2a'** is probably formed by a carba-Michael reaction of **2a** with surplus ethyl acrylate [31].

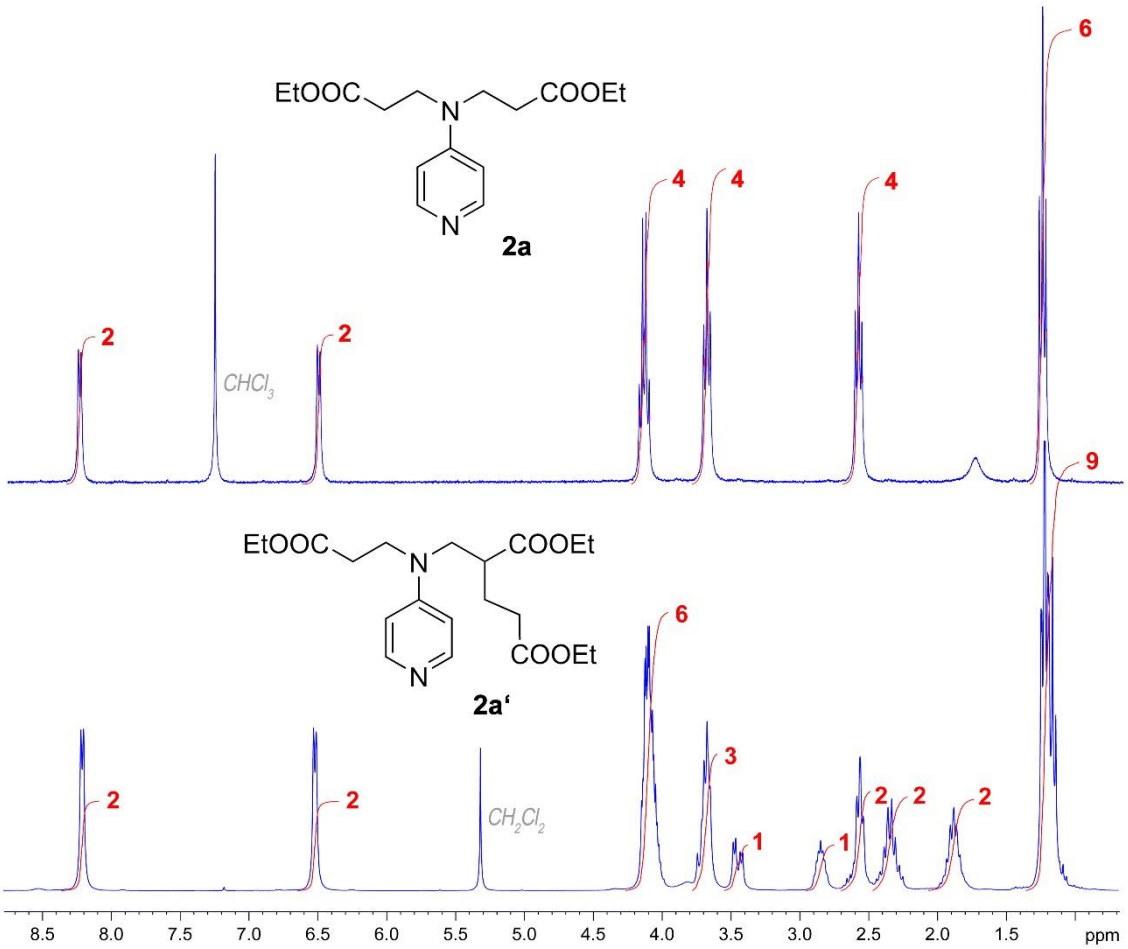

Figure 1. ^{1}H-NMR spectra of **2a** and **2a'** recorded in $CDCl_3$ at 300 MHz; the red numbers correspond to the integrals of the peaks.

It is interesting to note that no related byproducts were observed when imidazoles were used as Michael donors under similar reaction conditions [32]. The product of the double Michael addition of ethyl acrylate to 1,2,3,4-tetrahydropyrido[3,4-b]pyrazine (**2b**) is obtained in a similar way. Again, column chromatography was used to purify the target compound, which was obtained in 40 % yield. The two diesters **2a** and **2b** were then reduced with lithium aluminum hydride to give the corresponding dialcohols **3a** and **3b** in 60 and 50 % yield respectively (Scheme 3).

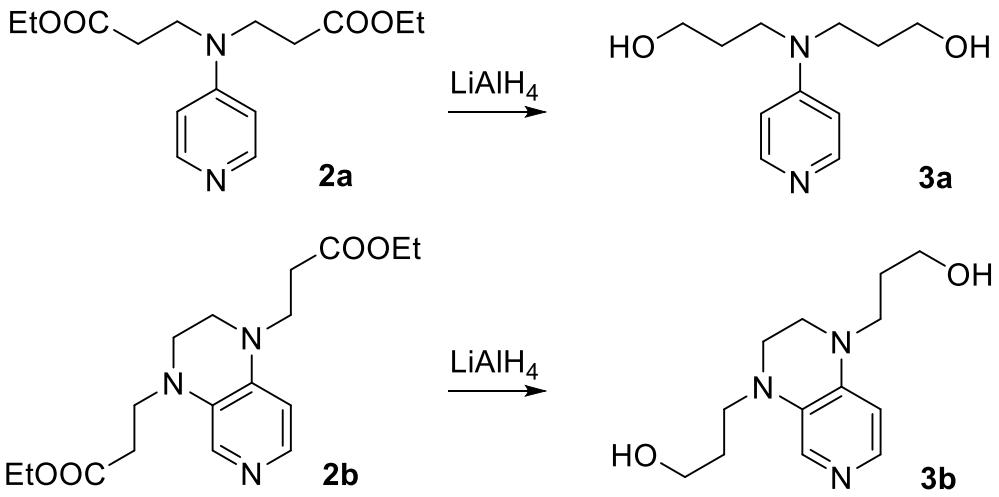

Scheme 3

In a next step, the synthesized electron-rich pyridine derivatives were tested as catalysts/initiators in the homopolymerization of phenyl glycidyl ether (PGE). The reaction was monitored using dynamic Differential Scanning Calorimetry (DSC) [10] accompanied by on-line monitoring of sample weights in a simultaneous thermal analysis (STA) instrument. The reaction has previously been studied under solvent-free conditions with a DMAP loading of 2 or 8 mol% [10]. However, the solubility of DMAP and the compounds prepared here in PGE at room temperature is only moderate and from our experience, loadings above 5 mol% are not fully soluble in the monomer within minutes at room temperature. The solubility of compounds **1b** and **2b** in PGE is particularly poor and therefore these two compounds were not evaluated in the following. Results are shown in Figure 2. The benchmark experiment with DMAP as the initiator shows an onset of the polymerization at about 80 °C, a maximum of the heat flow at 129±1 °C

and a heat of polymerization of about 96±3 kJ/mol. At the same time, a mass loss of 16±2 % is observed at a temperature of 210 °C, indicating that no complete polymerization of PGE could be obtained under these curing conditions. The cyanoethylated compound **1a** shows a much later onset of the polymerization (as indicated by the exothermic heat flow in the thermogram) at about 125 °C. Shortly before this, at about 118 °C, an endothermic event is observed, which could be due to the melting of undissolved crystals of **1a** (indeed, the solubility of **1a** in PGE is the lowest of all the molecules studied). The heat flux peaks at 141±1 °C and probably a lower heat of polymerization was evolved (> 80 kJ/mol, the simultaneous occurrence of an endothermic heat flux prevents a more accurate quantification) than in the case of DMAP. However, the mass loss observed in this experiment is very similar (16±2 % at 210 °C) to that found in the DMAP experiment, suggesting similar PGE conversions in both cases. In the case of the diethyl ester derivative **2a**, the onset of polymerization is found at a temperature about 20 °C lower than in the case of **1a**, but still considerably higher than in the case of DMAP. The heat flux has its maximum at about 136±1 °C and the heat of reaction is much lower at 70±3 kJ/mol, which is accompanied by a much higher mass loss of about 30±1 % at 210 °C. It is interesting to note that the mass loss already starts at about 100 °C, i.e. at a much lower temperature than in the case of DMAP or **1a**. Based on the literature [11-15], transesterification can be assumed to occur simultaneously with the anionic polymerization of PGE, which slows down the propagation reaction. A similar situation is conceivable for **1a**, where the attack of the alkoxide on the electrophilic carbon atom of the nitrile may slow the propagation. Finally, diol derivatives **3a** and **3b** show an early onset of the polymerization (similar to that of DMAP), but almost no heat of polymerization (in the range of 7-14 kJ/mol) could be detected. Instead, almost 80% mass loss was observed at 215 °C in the case of **3a** and even 85% in the case of **3b**, indicating the occurrence of deactivation reactions at elevated temperatures (becoming important above 110 °C) specific to these two pyridine derivatives. Deactivation of DMAP during homopolymerization has been described in the literature. It is believed, that the propagating ion pair (or zwitterion) is irreversibly consumed by the attack of an alkoxide on the π-system of a pyridinum cation (vide infra) [10,11]. Since in the case of **3a** and **3b** the alcohol groups are in close

proximity to the pyridinium moiety, it is easily conceivable that such degradation is more favored than in the case of DMAP or derivatives **1a** and **2a**.

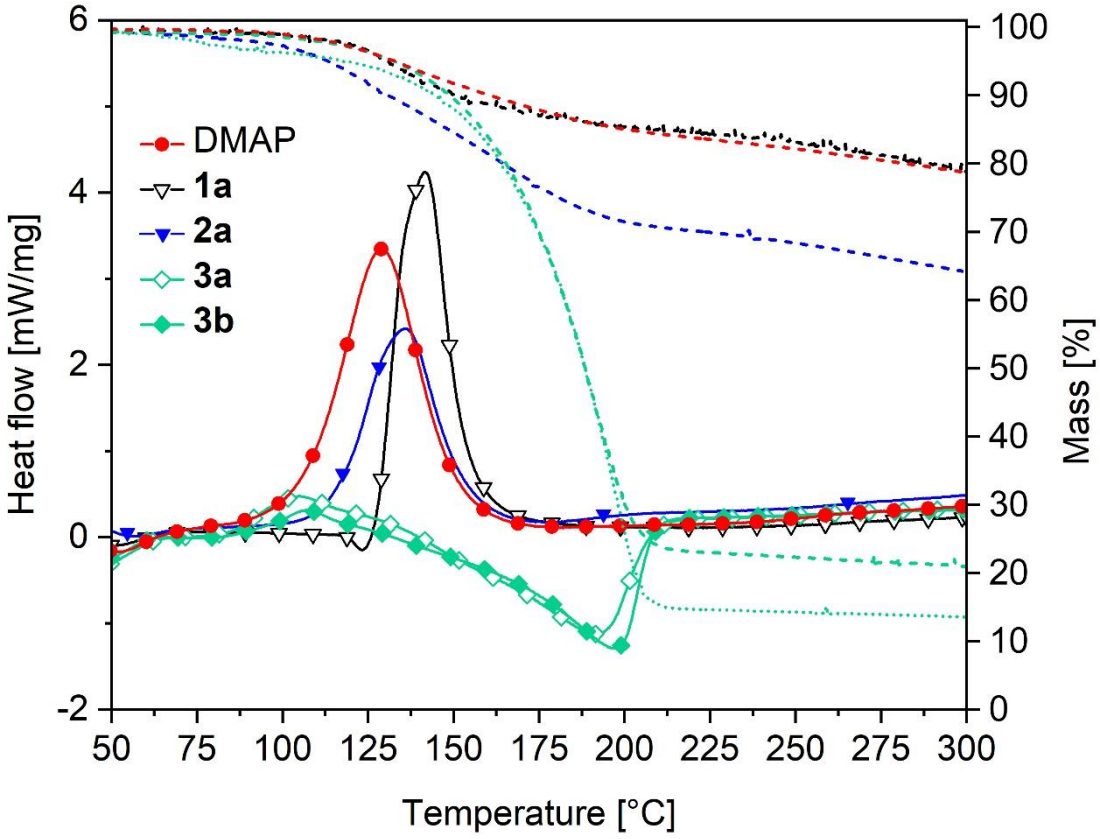

Figure 2. Dynamic STA measurements of the homopolymerization of PGE initiated with **1a**, **2a**, **3a**, **3b** and DMAP (5 mol% in respect to PGE; heat rate = 10 K/min) showing the heat flow of DSC experiments (thick lines with symbols, exothermal reactions show a positive heat flow) and the masses of the samples in dependence of the temperature (dashed lines with the same color code).

To further qualify the different initiators, isothermal curing of PGE in the presence of 5 mol% initiator at a fixed temperature of 100 °C (temperature chosen in the range where **3a** and **3b** still showed heat release in the previous experiments) was studied by DSC (Figure 3). Under these conditions, **3a** and especially the slightly better PGE soluble **3b** clearly outperformed DMAP and the other newly introduced derivatives **1a** and **1b**. Initiator **3b** shows a very fast PGE polymerization as indicated by the maximum heat flux at only 3±½ min and a heat of polymerization of 84±2 kJ/mol. **3a** behaves similarly (observed heat of reaction 83.5±2 kJ/mol), but the shape of the thermogram differs from the expected shape due to the presence of an additional endothermic event (probably melting of crystalline **3a**).

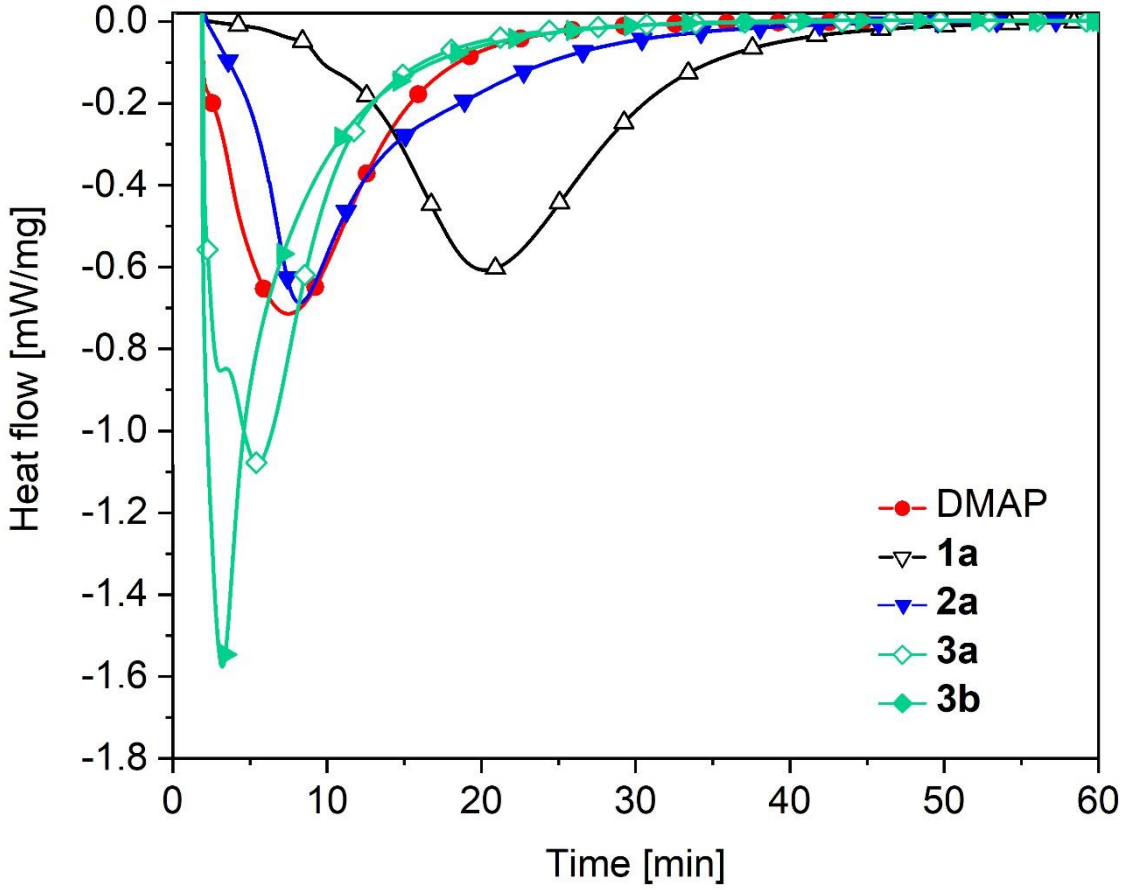

Figure 3. Isothermal DSC measurements of the homopolymerization of PGE initiated with **1a**, **2a**, **3a**, **3b** and DMAP (5 mol% in respect to PGE; reaction temperature: 100 °C) showing the heat flow (exothermal events show a negative heat flow)

The heat of reaction reported for the polymerizations initiated with **3a** and **3b** can be considered as the lower limits and are most probably higher (because considerable heat of polymerization could have developed during the first 2 min of the measurement, which is needed to reach the constant temperature of 100 °C). DMAP is giving a slower reaction as can be seen from the time taken to reach the maximum heat flux of about 6 min, and the heat of polymerization is with 68±2 kJ/mol lower than for **3a** or **3b**. Apparently, the alcohol groups attached to the electron-rich pyridine derivatives are advantageous for a fast conversion of PGE, which is in agreement with previous findings in the literature [11]. The reaction initiated by **2a** starts slightly slower than in the DMAP case, and takes significantly longer to complete the polymerization. A heat of polymerization of 72±2 kJ/mol was measured in this case. Finally, **1a** is by far the slowest initiator, showing a maximum heat flow at about 22 min. However, the highest PGE conversion was observed, as the highest heat of polymerization (90±2 kJ/mol)

was determined in this case. The nitrile groups appear to have some mitigating effect on the irreversible termination reaction.

To test the derivatives in an alcohol-rich environment, the curing of glycerol diglycidyl ether (gly-DGE, glycerol with an average of 1.5 glycidyl ether groups) with (Z)-but-2-ene-1,4-diol (molar ratio 1:1), as an exemplary epoxy alcohol formulation, was performed [33].

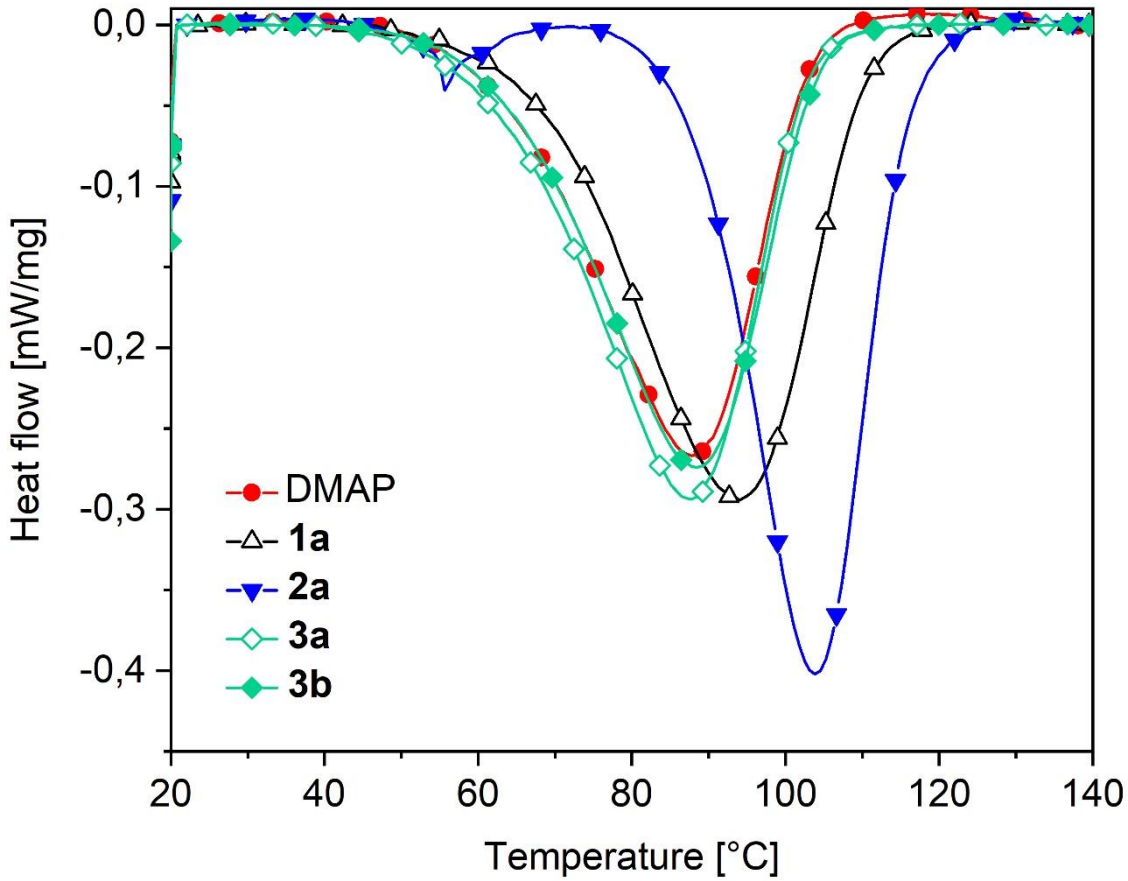

Figure 4. Dynamic DSC measurements of the epoxy alcohol reaction of Gly-DGE and (E)-but-2-ene-1,4-diol (molar ratio = 1:1) initiated with **1a**, **2a**, **3a**, **3b** and DMAP (5 mol% in respect to PGE; heat rate = 2 K/min) showing the heat flow of DSC experiments (exothermal reactions show a negative heat flow)

Under these conditions, **3a** and **3b** perform similarly to DMAP in terms of the onset of the polymerization (46±2 °C) and the maximum of the thermograms at (88±1 °C). However, the detected heat of polymerization is slightly lower for DMAP (42±2 kJ/mol) compared to **3a** and **3b** (45±2 kJ/mol). **1a** shows a slightly delayed polymerization (maximum at 97±1 °C) with a slightly higher heat of reaction (49±2 kJ/mol) compared to the previous cases. The diester derivative **2a** shows a different polymerization behavior. While the onset of the exothermic heat

flow is at a similar temperature as in the other cases, only a small amount of heat (< 3 kJ/mol) is released. Starting at about 74±1 °C, a second much stronger exothermic heat flux (46±2 kJ/mol) is observed, peaking at about 104±1 °C. The results show that the newly introduced alcohol-containing compounds **3a** and **3b** do not perform better than the parent DMAP in the epoxy-alcohol reaction. Considering that the theoretical heat of epoxy (homo)polymerization as well as epoxy-alcohol polymerization is about 100 kJ/mol [33,34] it can be concluded that under the experimental conditions all investigated derivatives are deactivated before the monomers are completely consumed and only epoxy conversions of about 50 % were obtained. The results show that in the presence of excess hydroxyl groups, all reactions are irreversibly terminated before the epoxy groups are consumed.

The results obtained allow to outline a better mechanistic understanding, in particular with respect to the role of the alkoxide in DMAP initiated epoxy polymerizations. First, DMAP reacts with an epoxy monomer in an equilibrium reaction to form the zwitterionic species **I** (Scheme 4). In the absence of alcohol, the alkoxide group in **I** can attack another PGE leading to propagation as illustrated by the homologous zwitterion **II**. In the presence of alcohols, the zwitterion **I** is removed from the equilibrium by a proton transfer reaction to form the ion-pair **III**, consisting of a pyridinium cation and an alkoxide, which then attacks another PGE molecule (**IV**) starting the propagation. The ion-pair pathway then allows a faster conversion of PGE, presumably simply because the concentration of active species (the alkoxide) is higher in this case [35]. The superior activity of **3a** and **3b** under isothermal curing conditions (at 100 °C) can therefore be rationalized by a switch from the zwitterionic to the ion pair pathway (Scheme 4, note that in the case of **3a** or **3b** and the ion pair pathway, the propagating species can be a zwitterion). Propagation can be terminated in a number of ways that cancel out the charges. Most of the termination reactions discussed involve hydrogen abstraction (β-elimination) and nucleophilic substitution by alkoxides (not shown in Scheme 4) [35]. These two processes release the Lewis base and allow the polymerization to be restarted as long as unreacted epoxy groups are present [11,36].

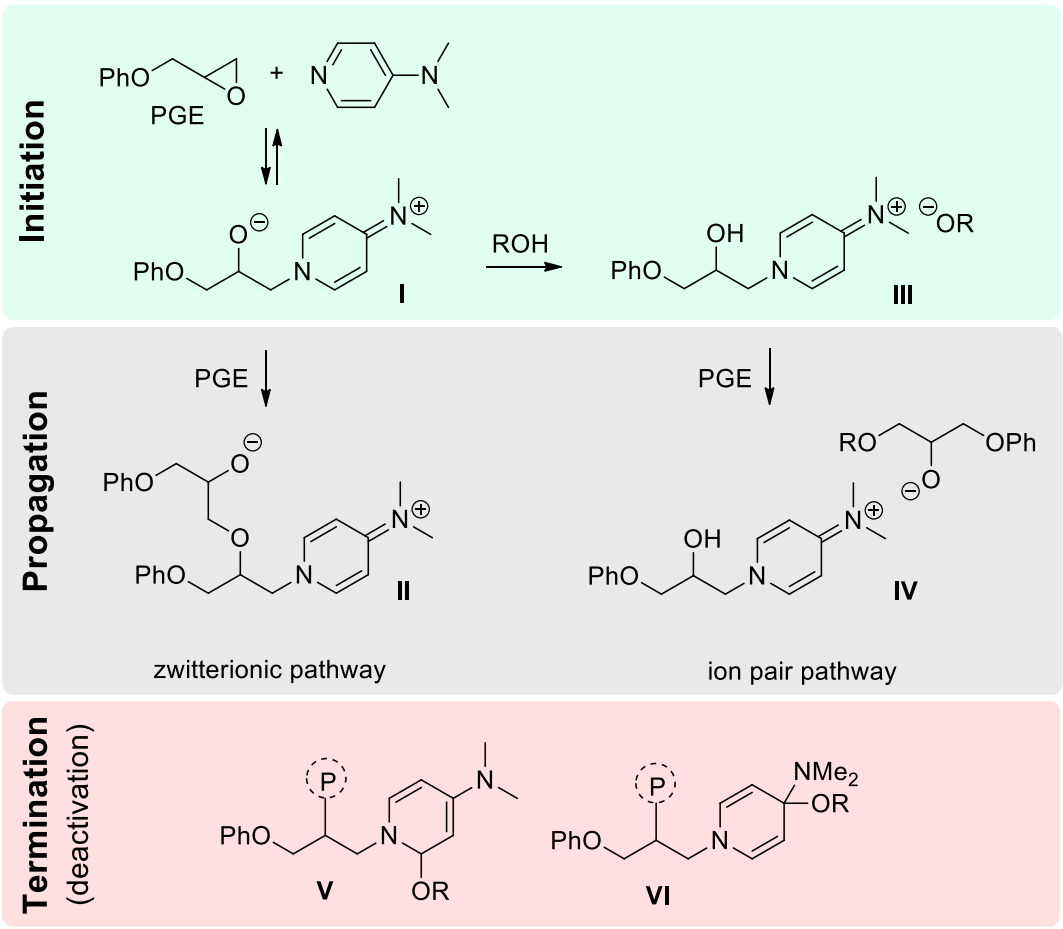

Scheme 4. (P in the dotted circle represents the polymer chain)

However, as seen previously [10] and in this study, DMAP derivatives undergo additional termination reactions leading to deactivation of the Lewis base in the presence of alkoxide. It has been suggested that the formation of species represented by **V** (intra- or intermolecular attack of the alkoxide on the pyridinium cation may occur) is responsible for the irreversible termination of the epoxy homopolymerization [10]. Such a deactivation reaction becomes more important at temperatures above 100 °C and the more alkoxide species are present. In case of hydroxyl group bearing **3a** and **3b**, the decomposition in an epoxy-homopolymerization is rapid above 100 °C resulting in the termination of PGE consumption. Figure 5 outlines a hypothetical scenario for **3a** that attempts to explain the decomposition reaction based on the reactivity of pyridinum ions [37]. Upon initiation, the zwitterion **Ia** is formed [38], which is in equilibrium with the zwitterion **IIIa**, which in turn may undergo an intramolecular cyclisation reaction to give the neutral **VIa**. Previously postulated species of type **V** [10], such as **Va** sketched here, should be less important for the irreversible termination of the

reaction, according to the findings made here. This is supported by the fact that the deactivation of the polymerization of PGE is fastest at elevated temperatures with the initiators **3a** and **3b** bearing alcohol groups. For these two compounds, intramolecular attack in the α-position to the nitrogen atom in the pyridinium ring is unlikely for steric reasons. DFT calculations of the relative energies of the structures **Ia**-**VIa** in comparison to the starting materials show no significant thermodynamic preference of one of the investigated structures.

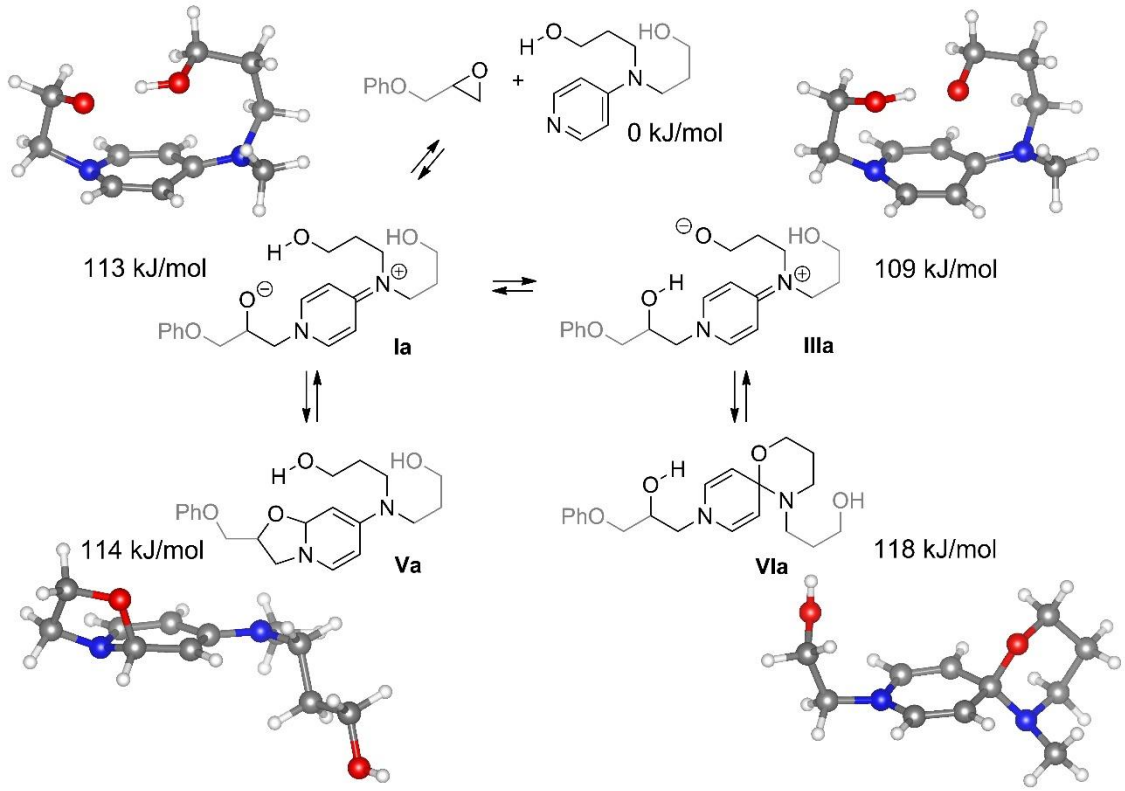

Figure 5 Chemical structures of the postulated zwitterions **Ia** and **IIIb** and potential reaction pathways leading to neutral molecules **Va** and **VIa**. Grey parts of the structures illustrate the parts of the molecules that were omitted in the calculations to reduce computational cost. Relative energies of **Ia**-**VIa** in respect to the respective starting materials and lowest-energy conformers of the calculated model structures are shown. All calculations were performed using B3LYP.

Furthermore, due to the relatively high energy differences observed, **Va** or **VIb** should rather be considered intermediates than final products of the attack of the alkoxide at the pyridinium moiety. We expect these intermediates to be starting points for yet unknown follow up reaction leading to thermodynamically more favored products and thus, the deactivation of the anionic polymerization reaction. The decomposition reaction starting from **Ia** to give **Va** should be equally feasible

for all studied DMAP derivatives and formation of the five-membered ring structure present in **Va** should be preferred over the formation of higher macrocycles or an intermolecular reaction. Accordingly, we postulate that the alkoxide attack on the other electrophilic carbon leading type **VIa** molecules, is at least another reasonable starting point for the irreversible termination of DMAP derivative promoted epoxy-homopolymerizations and epoxy-alcohol reactions. This pathway might be particularly important for the deactivation of **3a** and **3b** in the epoxy-homopolymerization at temperatures above 100 °C.

Conclusion

The aza-Michael reaction enables a simple and modular alkylation reaction of aminopyridine derivatives, introducing functional groups in the periphery of the electron-rich pyridine core. The presence of hydroxyl groups in the initiator is of particular interest because it provides a faster homopolymerization of phenyl glycidyl ether at 100°C than the parent 4-dimethylaminopyridine. However, epoxy homopolymerization and the epoxy alcohol reaction initiated with all electron-rich pyridine derivatives under investigation are irreversibly terminated at temperatures above 100°C. The termination reaction is particularly rapid at higher alcohol concentrations.

Experimental

Chemicals were purchased from Sigma-Aldrich, Fisher Scientific, Merck, or Alfa Aesar. All reagents were used without further purification unless otherwise noted. 1,2,3,4-Tetrahydropyrido[3,4-b]pyrazine was prepared according to literature [24]. NMR spectra were recorded on a Bruker Avance III 300 MHz FT NMR spectrometer (300.36 MHz (^{1}H), 75.53 MHz (^{13}C)). Chemical shifts δ [ppm] are referenced to residual protonated solvent signals as internal standard $CDCl_3$: δ = 7.26 ppm (^{1}H), 77.16 ppm (^{13}C). Elemental analyses were conducted on an Elementar Vario Micro Cube with CHN detector. Results were found to be in good agreement (±0.3%) with calculated values. Analytical thin layer chromatography (TLC) was performed on Merck silica gel 60-F_{254}, and spots were

visualized by UV-light or by treatment with cerium ammonium molybdate solution or potassium permanganate. Column chromatography was performed using silica gel 60 Å from Acros Organics. Thermogravimetric analysis (TGA) was performed with a Netzsch simultaneous thermal analyzer STA 449C (crucibles: aluminum from Netzsch). The heating rate was 10 °C/min until a final temperature of 550 °C was reached. A helium flow of 20 $cm^3 \cdot min^{-1}$ was used in combination with a protective flow of helium of 10 $cm^3 \cdot min^{-1}$. Differential scanning calorimetry (DSC) measurements were performed on a PerkinElmer DSC 8500 instrument using aluminum sealed pans. In case of dynamic measurements, the heat of polymerization (ΔH_0) was determined from the integration of the peak area of the corresponding thermogram according to Eq. 1.

$$\Delta H_0 \left[\frac{kJ}{mol}\right] = \frac{peak\ area \left[\frac{mW}{mg} * K\right]}{heat\ rate \left[\frac{K}{s}\right]} * \frac{m_{epoxy} + m_{alcohol} + m_{cat}\ [mg]}{Nr\ of\ epoxides\ [mmol]} / 1000 \qquad \text{(Eq. 1)}$$

In case of isothermal measurements, the heat of polymerization (ΔH^0) was determined from the integration of the peak area of the corresponding thermogram according to Eq. 2.

$$\Delta H_0 \left[\frac{kJ}{mol}\right] = peak\ area \left[\frac{mW}{mg} * min\right] * \frac{m_{epoxy} + m_{cat}\ [mg]}{Nr\ of\ epoxides\ [mmol]} * \frac{60}{1000} \quad \text{(Eq. 2)}$$

Computational Details

Conformational searches of all structures have been performed with the COSMO-conf programme (COSMOlogic GmbH & Co KG: Leverkusen, Germany, 2013) at the PBE-D3/def2-SVPD level [39,40]. The lowest energy structures were then reoptimized using PBE-D3/def2-SVPD as implemented in ORCA (version 5.0.2) [41]. Confirmation of the minima, calculation of zero-point vibrational energies and thermal properties (at 25 °C) were performed by calculation of analytical normal modes using the rigid-rotor harmonic oscillator (RRHO) approximation. The structures were used as input geometries for further optimization using the double-hybrid functional B3LYP-D3, the def2-TZVPPD basis set and D3 dispersion correction [42,43]. Our best estimate for calculation of Gibbs free energies (ΔG) resulted in using B3LYP-D3/def2-TZVPPD + ZPE,temp (PBE-

D3/def2-SVPD). Gibbs free energies were obtained by calculating the energy differences between products and starting materials.

3,3′-(4-Pyridinylimino)bis[propanenitrile] (**1a**)

A mixture of 4-aminopyridine (1.88 g, 0.020 mol) and acrylonitrile (13 cm^3, excess) was stirred for 24 h at 80 °C. The formed participate was filtered off, washed with acetone and dried in vacuum giving 2.73 g (68 %) of a white solid. R_f (CH_2Cl_2/MeOH = 20/1) = 0.21; ^{1}H-NMR (300 MHz, DMSO-d_6, 25 °C): δ = 8.16 (d, 2H, $^3J_{HH}$ = 6.5 Hz, py^{2,6}), 6.79 (d, 2H, $^3J_{HH}$ = 6.5 Hz, py^{3,5}), 3.74 (t, 4H, NCH_2CH_2), 2.76 (t, 4H, CH_2CH_2CN) ppm. ^{13}C{^{1}H}-NMR (75 MHz, DMSO-d_6, 25°C): δ = 151.1 (1C, py^4), 149.9 (2C, py^{2,6}), 119.1 (1C, N≡*C*-), 107.1 (2C, py^{3,5}), 44.6 (2C, NCH_2CH_2), 15.1 (2C, CH_2*C*H_2CN) ppm.

3,3′-(2,3-dihydropyrido[3,4-b]pyrazine-1,4-diyl)bis[propanenitrile] (**1b**, $C_{13}H_{15}N_5$)

A mixture of 1,2,3,4-tetrahydropyrido[3,4-b]pyrazine (200 mg, 1.48 mmol) and acrylonitrile (1 cm^3, excess) was stirred for 24 h at 80°C. Volatiles were removed in vacuum and the resulting oily brown residue was then purified by column chromatography (CH_2Cl_2/MeOH/TEA = 1500/100/1) on silica to afford upon drying in vacuum 218 mg (61 %) of a yellow solid. R_f = (CH_2Cl_2/MeOH/TEA = 1000/100/1) = 0.30; ^{1}H-NMR (300 MHz, $CDCl_3$, 25 °C): δ = 7.87 (d, 1H, $^3J_{HH}$ = 6 Hz, py^7), 7.67 (s, 1H, pyr^5), 6.31 (d, ^{1}H, $^3J_{HH}$ = 6 Hz, pyr^8), 3.65 (m, 4H, NCH_2CH_2), 3.60, 3.45 (m, 4H, pyr^{2,3}), 2.65 (m, 4H, CH_2CH_2CN) ppm. ^{13}C{^{1}H}-NMR (75 MHz, $CDCl_3$, 25°C): δ = 141.6, 139.7, 131.6, 129.4 (4 C, pyr^{4a,5,7,8a}), 118.3, 117.9 (2C, CH_2CH_2*C*N), 104.5 (1C, pyr^8), 48.0, 47.1, 46.8 (4C, pyr^{2,3}, *C*H_2CH_2CN), 15.1 (2C, CH_2*C*H_2CN) ppm.

N-(3-Ethoxy-3-oxopropyl)-*N*-4-pyridinyl-β-alanine ethyl ester (**2a**)

A mixture of 4-aminopyridine (1.88 g, 0.020 mol) and ethyl acrylate (11 cm^3, excess) were stirred at 80°C for 24 h. Volatiles were removed in vacuum and the brown oily crude material was purified with column chromatography (CH_2Cl_2/MeOH/TEA = 90/10/1) on silica to afford a light brown solid (2.53 g, 43 %).

R_f (CH_2Cl_2/MeOH/TEA = 90/10/1) = 0.45; ^{1}H-NMR (300 MHz, $CDCl_3$, 25 °C): δ = 8.24 (d, 2H, $^3J_{HH}$ = 5 Hz, py^{2,6}), 6.51 (d, 2H, $^3J_{HH}$ = 5 Hz, py^{3,5}), 4.15 (q, 4H, $^3J_{HH}$ = 7 Hz, OCH_2CH$_3$), 3.69 (t, 4H, $^3J_{HH}$ = 7 Hz, CH$_2$CH_2N), 2.59 (t, 4H, $^3J_{HH}$ = 7 Hz, CH_2CH$_2$N), 1.25 (t, 6H, $^3J_{HH}$ = 7 Hz, OCH$_2$CH_3) ppm. ^{13}C{^{1}H}-NMR (75 MHz, $CDCl_3$, 25°C): δ = 171.6 (2C, *C*OO), 151.8 (1C, py^4), 150.3 (2C, py^{2,6}), 106.9 (2C, py^{3,5}), 61.0 (2C, O*C*H$_2$CH$_3$), 45.9 (2C, CH$_2$*C*H$_2$N), 32.3 (2C, *C*H$_2$CH$_2$N), 14.3 (2C, OCH$_2$*C*H$_3$) ppm.

Diethyl 2-(((3-ethoxy-3-oxopropyl)(pyridin-4-yl)amino)methyl)pentanedioate ($C_{20}H_{30}N_2O_6$, **2a'**)

2a' was isolated from the reaction mixture obtained during the synthesis of **2a** by column chromatography giving upon drying in vacuum 180 mg (2.3 %) of a slightly yellow oil. R_f (CH_2Cl_2/MeOH/TEA = 90/10/1) = 0.50; ^{1}H-NMR (300 MHz, $CDCl_3$, 25 °C): δ = 8.23 (d, 2H, $^3J_{HH}$ = 5 Hz, py^{2,6}), 6.50 (d, 2H, $^3J_{HH}$ = 5 Hz, py^{3,5}), 4.19-3.99 (m, 6H, OCH_2CH$_3$), 3.75-3.60 (m, 3H, CH$_2$CH_2N, CHCH_2N), 3.42 (m, 1H, CHCH_2N), 2.83 (m, 1H, CH$_2$C*H*CH$_2$), 2.55 (t, 2H, CH_2CH$_2$N), 2.33 (m, 2H, CHCH$_2$CH_2COO), 1.89 (m, 3.9H, CHCH_2CH$_2$COO, 1.9H unknown), 1.31-1.11 (m, 9H, OCH$_2$CH_3) ppm. ^{13}C{^{1}H}-NMR (75 MHz, $CDCl_3$, 25°C): δ = 173.4, 171.9, 170.9 (3C, *C*OO), 151.4 (1C, py^4), 149.7 (2C, py^{2,6}), 106.6 (2C, py^{3,5}), 60.4, 60.2, 60.0 (3C, O*C*H$_2$CH$_3$), 51.8 (1C, CH*C*H$_2$N), 45.5 (1C, CH$_2$*C*H$_2$N), 42.7 (1C, *C*HCH$_2$N), 31.18, 31.13 (2C, *C*H$_2$CH$_2$), 24.7 (1C, CH*C*H$_2$CH$_2$COO), 13.71, 13.68, 13.63 (3C, OCH$_2$*C*H$_3$) ppm.

Diethyl 3,3'-(2,3-dihydropyrido[3,4-b]pyrazine-1,4-diyl)dipropionate (**2b**, $C_{17}H_{25}N_3O_4$)

2b was prepared analogously to **1b** using 1,2,3,4-tetrahydropyrido[3,4-b]pyrazine (0.80 g, 5.9 mmol) and ethyl acrylate (3.5 cm^3, excess) as the starting materials. Purification was accomplished by column chromatography (CH_2Cl_2/MeOH/TEA = 2500/100/1) on silica to afford a light brown solid (0.79 g, 40 %). R_f (CH_2Cl_2/MeOH/TEA = 1000/10/1) = 0.40; ^{1}H-NMR (300 MHz, $CDCl_3$, 25 °C): δ = 7.80 (d, 1H, $^3J_{HH}$ = 6 Hz, pyr^7), 7.67 (s, 1H, pyr^5), 6.36 (d, 1H, $^3J_{HH}$ = 6 Hz, pyr^8), 4.14 (q, 4H, $^3J_{HH}$ = 7 Hz, OCH_2CH$_3$), 3.59, (m, 4H, pyr^{2,3}), 3.47, 3.29 (m, 4H, NCH_2CH$_2$), 2.59 (m, 4H, NCH$_2$CH_2), 1.24 (t, 6H, $^3J_{HH}$ = 7 Hz, OCH$_2$CH_3) ppm. ^{13}C{^{1}H}-NMR (75 MHz, $CDCl_3$, 25°C): δ = 171.9 (2C, *C*OO), 141.8, 139.9,

131.5, 129.3 (4C, pyr[4a,5,7,8a]), 104.7 (1C, pyr[8]), 61.2 (2C, O*C*H$_2$CH$_3$), 48.2, 47.4, 46.3, 45.9 (4C, pyr[2,3], *C*H$_2$CH$_2$COO), 32.3, 32.1 (2C, CH$_2$*C*H$_2$COO), 14.3 (2C, OCH$_2$*C*H$_3$) ppm.

3,3'-(Pyridin-4-ylazanediyl)bis(propan-1-ol) (**3a**, $C_{11}H_{18}N_2O_2$)
To a suspension of lithium aluminum hydride (245 mg, 6.5 mmol) in THF (12 cm^3) at 0 °C, a solution of **2a** (1.14 g, 3.87 mmol) in THF (5 cm^3) was added dropwise over 10 min. The reaction mixture was vigorously stirred for 4 h at room temperature. Water was added dropwise to the stirred reaction mixture and the formed precipitate was filtered off and washed 3 times with THF (5 cm^3 each). The THF solution was dried over Na_2SO_4 and after evaporation of volatiles, a brown oily residue was obtained. The crude product was purified by recrystallization from acetonitrile (approx. 10 cm^3) releasing colorless crystals (0.49 g, 60 %). R_f (CH_2Cl_2/MeOH/TEA = 100/10/1) = 0.90; ^{1}H-NMR (300 MHz, $CDCl_3$, 25 °C): δ = 8.13 (d, 2H, $^3J_{HH}$ = 6 Hz, py[2,6]), 6.53 (d, 2H, $^3J_{HH}$ = 6 Hz, py[3,5]), 3.72 (q, 4H, $^3J_{HH}$ = 7 Hz, NCH$_2$CH$_2$C*H*$_2$O), 3.48 (t, 4H, $^3J_{HH}$ = 7 Hz, NC*H*$_2$CH$_2$CH$_2$O), 1.85 (m, 4H, NCH$_2$C*H*$_2$CH$_2$O) ppm. ^{13}C{^{1}H}-NMR (75 MHz, $CDCl_3$, 25°C): δ = 152.6 (1C, py[4]), 149.7 (2C, py[2,6]), 106.6 (2C, py[3,5]), 59.9 (2C, NCH$_2$CH$_2$*C*H$_2$O), 46.7 (2C, N*C*H$_2$CH$_2$CH$_2$O), 29.8 (2C, NCH$_2$*C*H$_2$CH$_2$O) ppm.

3,3'-(2,3-Dihydropyrido[3,4-b]pyrazine-1,4-diyl)bis(propan-1-ol) (**3b**, $C_{13}H_{21}N_3O_2$)
3b was prepared analogously to **3a** using lithium aluminum hydride (189 mg, 5 mmol) and **2b** (600 mg, 1.79 mmol) as the starting materials resulting in a white solid (225 mg, 50 %). R_f (CH_2Cl_2/MeOH/TEA = 1000/10/1) = 0.10; ^{1}H-NMR (300 MHz, $CDCl_3$, 25 °C): δ = 7.70 (d, 1H, $^3J_{HH}$ = 6 Hz, pyr[7]), 7.64 (s, 1H, pyr[5]), 6.60 (d, 1H, $^3J_{HH}$ = 6 Hz, pyr[8]), 3.65 (m, 4H, $^3J_{HH}$ = 6 Hz, NCH$_2$CH$_2$C*H*$_2$O), 3.47, 3.40, 3.25, 3.18 (m, 8H, pyr[2,3], NC*H*$_2$CH$_2$CH$_2$O), 1.82 (4H, m, NCH$_2$C*H*$_2$CH$_2$O) ppm. ^{13}C{^{1}H}-NMR (75 MHz, $CDCl_3$, 25°C): δ = 141.4, 140.7, 131.8, 130.9 (4C, pyr[4a,5,7,8a]), 104.2 (1C, pyr[8]), 61.0, 60.0 (2C, NCH$_2$CH$_2$*C*H$_2$O), 48.7, 47.5, 47.2, 46.1 (4C, N pyr[2,3], *C*H$_2$CH$_2$CH$_2$O), 28.9, 28.6 (2C, CH$_2$*C*H$_2$CH$_2$O) ppm.

Acknowledgements Financial support by the Austrian Federal Ministry for Digital and Economic Affairs, the National Foundation for Research, Technology

and Development, and the Christian Doppler Research Association (Christian Doppler Laboratory for Organocatalysis in Polymerization) is gratefully acknowledged. We thank A. Daniel Boese (University of Graz) for providing access to HPC resources.

References

1. Höfle G, Steglich W, Vorbrüggen H (1978) 4-Dialkylaminopyridines as Highly Active Acylation Catalysts. Angew Chem Int Ed 17:569-583 DOI: 10.1002/anie.197805691

2. Berry DJ, DiGiovanna CV, Metrick SS, Murugan R (2001) Arkivoc 201-226 DOI: 10.3998/ark.5550190.0002.114

3. Nederberg F, Connor EF, Möller M, Glauser T, Hedrick JL (2001) New Paradigms for Organic Catalysts: The First Organocatalytic Living Polymerization. Angew Chem Int Ed 40: 2712-2714 DOI: 10.1002/1521-3773(20010716)40:14<2712::AID-ANIE2712>3.0.CO;2-Z

4. Helberg J, Ampßler T, Zipse H (2020) Pyridinyl Amide Ion Pairs as Lewis Base Organocatalysts. J Org Chem 85: 5390–5402 DOI: 10.1021/acs.joc.0c00114

5. Edinger D, Weber H, Žagar E, Pahovnik D, Slugovc C (2021) Melt-polymerization of acrylamide initiated by nucleophiles: a route towards highly branched and amorphous polyamide 3. ACS Appl Polym Mater 3: 2018-2026 DOI: 10.1021/acsapm.1c00084

6. Ratzenböck K, Fischer SM, Slugovc C (2023) Poly(ether)s derived from oxa-Michael polymerization - A comprehensive review. Monatsh Chem 54: 443-458. DOI: 10.1007/s00706-023-03049-4

7. Strasser S, Wappl C, Slugovc C (2017) Solvent-free macrocyclisation by nucleophile-mediated oxa-Michael addition polymerisation of divinyl sulfone and alcohols. Polym Chem 8: 1797-1804 DOI: 10.1039/C7PY00152E

8. Ratzenböck K, Din MMU, Fischer SM, Žagar E, Pahovnik D, Boese AD, Rettenwander D, Slugovc C (2022) Water as a monomer: synthesis of an aliphatic polyethersulfone from divinyl sulfone and water. *Chem Sci 13*: 6920-6928 DOI: 10.1039/D2SC02124B

9. Ratzenböck K, Pahovnik D, Slugovc C (2020) Step-growth polymerisation of alkyl acrylates via concomitant oxa-Michael and transesterification reactions. Polym Chem 11: 7476-7480 DOI: 10.1039/D0PY01271H

10. Dell'Erba IE, Williams RJJ (2006) Homopolymerization of epoxy monomers initiated by 4-(dimethylamino)pyridine. Polym Eng Sci 46: 351-359 DOI: 10.1002/pen.20468

11. Fernández-Francos X, Cook WD, Serra A, Ramis X, Liang GG, Salla MJ (2010) Crosslinking of mixtures of DGEBA with 1,6-dioxaspiro[4,4]nonan-2,7-dione initiated by tertiary amines. Part IV. Effect of hydroxyl groups on initiation and curing kinetics. Polymer 51: 26-34 DOI: 10.1016/j.polymer.2009.11.013

12. Chen CH, Gu ZC, Tsai YL, Jeng RJ, Lin CH (2018) Identification of the reaction mechanism between phenyl methacrylate and epoxy and its application in preparing low-dielectric epoxy thermosets with flexibility. Polymer 140: 225-232 DOI: 10.1016/j.polymer.2018.02.045

13. Chen, B, Zhang, Q, Lu, M, Meng H, Qu Z, Xu C, Jiao E (2021) Synthesis of a novel lignin-based epoxy resin curing agent and study of cure kinetics, thermal, and mechanical properties. J Appl Polym Sci 138: e50523 DOI: 10.1002/app.50523

14. Shao SW, Chen CH, Chan JR, Juang TY, Abu-Omar MM, Lin CH (2020) Full atom-efficiency transformation of wasted polycarbonates into epoxy thermosets and the catalyst-free degradation of the thermosets for environmental sustainability. Green Chem 22: 4683-4696 DOI: 10.1039/D0GC01318H

15. Lin CM, Chen CH, Lin CH, Su WC, Juang TY (2018) Using Dicyclopentadiene-Derived Polyarylates as Epoxy Curing Agents To Achieve High Tg and Low Dielectric Epoxy Thermosets. ACS Omega 3: 4295-4305 DOI: 10.1021/acsomega.8b00256

16. Natongchai W, Luque-Urrutia JA, Phungpanya C, Solà M, D'Elia V, Poater A, Zipse H (2021) Cycloaddition of CO_2 to epoxides by highly nucleophilic 4-aminopyridines: establishing a relationship between carbon basicity and catalytic performance by experimental and DFT investigations. Org Chem Front 8: 613-627 DOI: 10.1039/D0QO01327G

17 Natongchai W, Posada-Pérez S, Phungpanya C, Luque-Urrutia JA, Solà M, D'Elia V, Poater A (2022) Enhancing the Catalytic Performance of Group I, II Metal Halides in the Cycloaddition of CO_2 to Epoxides under Atmospheric Conditions by Cooperation with Homogeneous and Heterogeneous Highly Nucleophilic Aminopyridines: Experimental and Theoretical Study. J Org Chem 87: 2873–2886 DOI: 10.1021/acs.joc.1c02770

18. Murayama M, Sanda F, Endo T (1998) Anionic Ring-Opening Polymerization of a Cyclic Carbonate Having a Norbornene Structure with Amine Initiators. Macromolecules 31: 919-923 DOI: 10.1021/ma970878j

19. Price KE, Mason BP, Bogdan AR, Broadwater SJ, Steinbacher JL, McQuade DT (2006) Microencapsulated Linear Polymers: "Soluble" Heterogeneous Catalysts. J Am Chem Soc 128: 10376–10377 DOI: 10.1021/ja063688+

20. D'Elia V, Liu Y, Zipse H (2011) Immobilized DMAP Derivatives Rivaling Homogeneous DMAP. Eur J Org Chem 1527-1533 DOI: 10.1002/ejoc.201001507

21. Rulev AY (2023) Aza-Michael Reaction: A Decade Later – Is the Research Over? Eur J Org Chem DOI: 10.1002/ejoc.202300451

22. Shimizu S, Watanabe N, Kataoka T, Shoji T, Abe N, Morishita S, Ichimura H (2007) Pyridine and Pyridine Derivatives in Ullmann's Encyclopedia of Industrial Chemistry. Weinheim: Wiley-VCH. DOI: 10.1002/14356007.a22_399

23. Garavaglia F, Barozza A, Roletto J, Paissoni P (2011) One-pot process for preparation of dalfampridine. European Patent 2394994 A1 Dec 14, 2011.

24. Held I, Xu S, Zipse H (2007) Modular Design of Pyridine-Based Acyl-Transfer Catalysts. Synthesis 10: 1185–1196 DOI: 10.1055/s-2007-965973

25. Ni J, Li Y-Z, Qi, W-B, Liu, Y-J, Chen, H-L, Wang, Z-L (2003) 4-[N,N-Bis(2-cyano-ethyl)-amino]-pyridine. Acta Crystallogr C Cryst Struct, C59: o470-o472 DOI: 10.1107/S0108270103012630

26. Buckus P, Buckiene A (1963) Cyanoethylation of 4-aminopyridine. Zhurnal Obshchei Khimii 33: 3112-3113 Chem Abstr 123:56613

27. Huang J, Sun, J, Cao A, Liu Z, Shao S (1994) Synthesis of novel alkylaminopyridine monomers as high-performance acylation catalysts. Huaxue Shijie 35: 188-190 Chem Abstr 60:9635

28. Nishida H (2003) Preparation of 1-(4-pyridyl)-4-piperidone. World Patent 2003095446 A1 Nov 20, 2003 Chem Abstr 139:364837

29. Delaney EJ, W LE, Klotz IM (1982) Poly(ethylenimines) with alternative (alkylamino)pyridines as nucleophilic catalysts. J Am Chem Soc 104: 799-807 DOI: 10.1021/ja00367a025

30. Klotz IM, Massil SE, Wood LE (1985) Poly(aminopyridine)s. J Polym Sci Polym Chem Ed 23: 575-579 DOI: 10.1002/pol.1985.170230230

31. Fischer SM, Schallert V, Uher JM, Slugovc C (2023) *Polym Chem 14*: 1081-1084. DOI: 10.1039/D3PY00035D

32. Kodolitsch K, Gobec F, Slugovc C (2020) Solvent- and catalyst-free aza-Michael addition of imidazoles and related heterocycles. *Eur J Org Chem 19*: 2973-2978 DOI: 10.1002/ejoc.202000309

33. Fantoni A, Koch T, Baudis S, Liska R (2023) Synthesis and Characterization of Homogeneous Epoxy Networks: Development of a Sustainable Material Platform Using Epoxy-Alcohol Polyaddition. ACS Appl Polym Mater 5: 731–742 DOI: 10.1021/acsapm.2c01728

34. Rozenberg BA (1986) Kinetics, thermodynamics and mechanism of reactions of epoxy oligomers with amines. Adv Polym Sci 75: 113–65 DOI: 10.1007/bfb0017916

35. Fernàndez-Francos X (2014) Theoretical modeling of the effect of proton donors and regeneration reactions in the network build-up of epoxy thermosets using tertiary amines as initiators. Eur Polym J 55: 35-47 DOI: 10.1016/j.eurpolymj.2014.03.022

36. Fernández-Francos X, Konuray A-O, Belmonte A, De la Flor S, Serra À, Ramis X (2016) Sequential curing of off-stoichiometric thiol–epoxy thermosets with a custom-tailored structure. Polym Chem 7: 2280-2290 DOI: 10.1039/C6PY00099A

37. Kratena N, Marinic B, Donohoe TJ (2022) Recent advances in the dearomative functionalisation of heteroarenes. Chem Sci 13: 14213-14225 DOI: 10.1039/D2SC04638E

38. Lam Y-P, Wang X, Tan F, Ng W-H, Tse Y-LS, Yeung Y-Y (2019) Amide/Iminium Zwitterionic Catalysts for (Trans)esterification: Application in Biodiesel Synthesis. ACS Catal 9: 8083-8092 DOI: 10.1021/acscatal.9b01959

39. Perdew JP, Burke K, Ernzerhof M (1996) Generalized Gradient Approximation Made Simple. Phys Rev Lett. 77: 3865-3868 DOI: 10.1103/PhysRevLett.77.3865

40. Grimme S, Antony J, Ehrlich S, Krieg H (2010) A consistent and accurate ab initio parametrization of density functional dispersion correction (DFT-D) for the 94 elements H-Pu. J Chem Phys 132: 154104 DOI: 10.1063/1.3382344

41. Neese F (2018) Software update: the ORCA program system, version 4.0 Wiley Interdiscip Rev Comput Mol Sci 8: e1327 DOI: 10.1002/wcms.1327

42. Becke AD (1988) Density-functional exchange-energy approximation with correct asymptotic behavior. Phys Rev A 38: 3098-3100 DOI: 10.1103/PhysRevA.38.3098

43. Grimme S (2006) Semiempirical hybrid density functional with perturbative second-order correlation. J Chem Phys 124: 034108 DOI: 10.1063/1.2148954